

RELATING FACIES CONNECTIVITY TO FLOW AND TRANSPORT PROPERTIES FOR A POINT BAR-CHANNEL AQUIFER ANALOGUE

Diana dell’Arciprete^{*}, Fulvia Baratelli^{♦*}, Riccardo Bersezio[◇], Fabrizio Felletti[◇],
Mauro Giudici^{*} and Chiara Vassena^{*}

^{*} Università degli Studi di Milano, Dipartimento di Scienze della Terra “A. Desio”
Sezione di Geofisica
via Cicognara 7, 20129 Milano, Italy
e-mail: diana.dellarciprete@unimi.it, mauro.giudici@unimi.it, chiara.vassena@unimi.it

[♦] Università degli Studi di Milano, Dipartimento di Fisica
via Celoria 16, 20133 Milano, Italy
e-mail: fulvia.baratelli@unimi.it

[◇] Università degli Studi di Milano, Dipartimento di Scienze della Terra “A. Desio”
Sezione di Geologia e Paleontologia
via Mangiagalli 34, 20133 Milano, Italy
e-mail: riccardo.bersezio@unimi.it, fabrizio.felletti@unimi.it

Key words: Ground water, alluvial aquifers, aquifer analogues, connectivity, transport.

Summary. An aquifer analogue in historical sediments of a meandering river in the Po plain (Northern Italy) was studied with a multidisciplinary approach (geology, geostatistical simulation, flow and transport modeling). Ensembles of realizations obtained with different geostatistical methods were used to analyze the connectivity indicators and the flow and transport parameters so that information on the hydrodynamic and hydrodispersive behavior of point bar-channel aquifers can be inferred.

1 INTRODUCTION

Facies connectivity is one of the most influent parameters on groundwater flow paths and on solute transport at any scale. In alluvial aquifers, the degree of connection among facies bodies contributes to determine flow path and velocity, convection and dispersion of contaminants. For this reason the quantification of connectivity at different scales could provide constraints for the simulation of aquifer heterogeneity and to improve the development and application of models of ground water flow and contaminant transport. To explore this opportunity we studied a well-exposed and well-known aquifer analogue, at the scale of the point-bar/channel depositional element of a meandering river.

The analogue, exposed in a gravel pit, is part of the historical sediments of the terraced meandering valley of the Lambro River (Po plain, Northern Italy). Previous works included the development of the geological model (geometry, hierarchy and internal architecture of the

sedimentary bodies)^{1,6}, the geostatistical simulations of hydrofacies distribution³, a connectivity analysis⁴, the ground water flow modeling and some virtual experiments of a non reactive solute transport².

The whole volume under study (about 30000 m³) was simulated on two different grids with three methods (SISIM, T-Progs and MPS), using conditioning data from five quarry faces. A test volume (about 370 m³) was simulated with SISIM and MPS at the hydrofacies scale.

The aim of this paper is to present the results of the connectivity analysis for the test volume, so that some preliminary comments on the link between connectivity indicators and transport properties can be drawn. In particular an ensemble of equiprobable realizations for each simulation method permits, in a Monte Carlo fashion, to compute the probability density functions of indicators of facies connectivity¹² and of the equivalent conductivity tensor and therefore of flow connectivity indicators¹⁰. Moreover, virtual field data on transport processes were generated by simulating the evolution of contaminant plumes through these portions of a virtual alluvial aquifer: one experiment of convective transport of a non-reactive solute was performed for each realization and each method, so that transport connectivity indicators¹² were computed. The analysis of the results, in particular the correlation between different connectivity indicators, permits further insight in the comprehension of the hydrodispersive parameters of point bar-channel aquifers.

2 THE HYDROSTRATIGRAPHIC AND GEOSTATISTICAL MODELS

For this study the historical sediments of the Lambro River are analyzed at a quarry site south of Milan (figure 1), where the Lambro River is a meandering river, flowing since the post-glacial age within a narrow valley encased into the Upper Pleistocene sandur of the Lecco glacial amphitheatre. The quarry site exposed three superimposed depositional units formed by sands, gravels and subordinate silt and clay, which could be attributed to an historical age, as it was proved by the findings of Roman to Middle Age and Renaissance Age artifacts (bricks, tiles, ceramics), imbricated within dunes and bars^{1,6}. Two units were recognized: unit A (the lower, with Roman-Middle Age findings) shows the lateral transition from composite point bar to channel fill; unit B (the upper, with Renaissance Age findings) is mostly represented by a composite point bar, with chute channels scoured and filled on top. A and B units are separated by an erosion surface (α), tapered by lag deposits. A younger channel (unit C, bounded by the erosion surface β and partly anthropogenic) eroded part of unit B. The three units (A, B and C) are cut by the modern and present-day courses of the Lambro river. Units A and B are formed by a hierarchic arrangement of depositional units, from the 2nd order of bed-sets to the 5th order of the bar/channel systems, which determines the architectural heterogeneity of the aquifer analogue.

The geological and hydrostratigraphic model was elaborated from the stratigraphical, sedimentological and geophysical analysis of the quarry volume. The field data included: i) facies maps of the quarry faces (four with an EW orientation and one with a SN orientation); ii) 31 vertical stratigraphic logs with cm-scale resolution along the five quarry faces; iii) grain-size, porosity and conductivity data of 28 samples; iv) ground penetrating radar and electrical resistivity images of the volume, providing additional 3D constraints to

the shape of the stratigraphic boundaries.

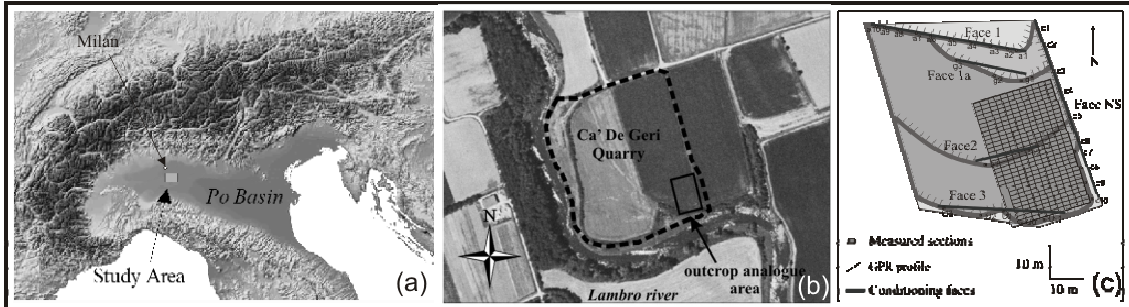


Figure 1: Location of the study area (a, b) and position of the vertical sections (c).

Facies mapping was performed in the field and was supported by the analysis of the photo-composition of the quarry faces: as a result plan-view and vertical maps of geometry and size of the different hierarchic elements was obtained together with a classification of 22 sedimentary facies, grouped into 5 facies classes. More in detail the geological and hydrostratigraphic model includes: i) the geometry and the hierarchic arrangement of the depositional units and of their bounding surfaces at different scales; ii) the distribution of the facies and the hydrofacies within the hierarchical arrangement of the stratigraphic units; iii) the hydrostratigraphical characterisation of the hydrofacies and the hydrofacies groups (porosity, permeability, continuity and connectivity); iv) the interpretation of the genesis and the evolution of the sedimentary bodies.

Then the volume was simulated with three geostatistical methods: SISIM^{8,11} (sequential indicator simulation), T-ProGS⁷ (Markov chain model of transitional probabilities) and MPS¹³ (multiple point simulation). Conditioning data were taken from the vertical facies maps of the five vertical sections, discretized with square cells (0.05 m spacing). For modelling purposes four hydrofacies were used, based on the analysis of *K* values obtained by samples: least permeable (F, very fine sand and silt-clay respectively from topmost channel-fill, silt/clay plugs, drapes and balls), low permeable (S, sand from point-bar and channel fill bedforms), medium permeable (SG, sandy gravel and gravelly sand from point bars) and most permeable (G, open framework gravels from the lower parts of the lateral accreted units).

In particular the test volume (11.4 m×11.4 m×2.85 m) was simulated with SISIM and MPS on a grid of voxels whose dimensions (0.2 m×0.2 m×0.05 m) are consistent with the hydrofacies representation and the field data density. An ensemble of 50 equiprobable realizations was obtained for each method. This test volume was chosen in an area where a lot of conditioning data belonging to two orthogonal faces were available and the three sedimentary units A, B and C were present. One realization for each method is shown in figure 2.

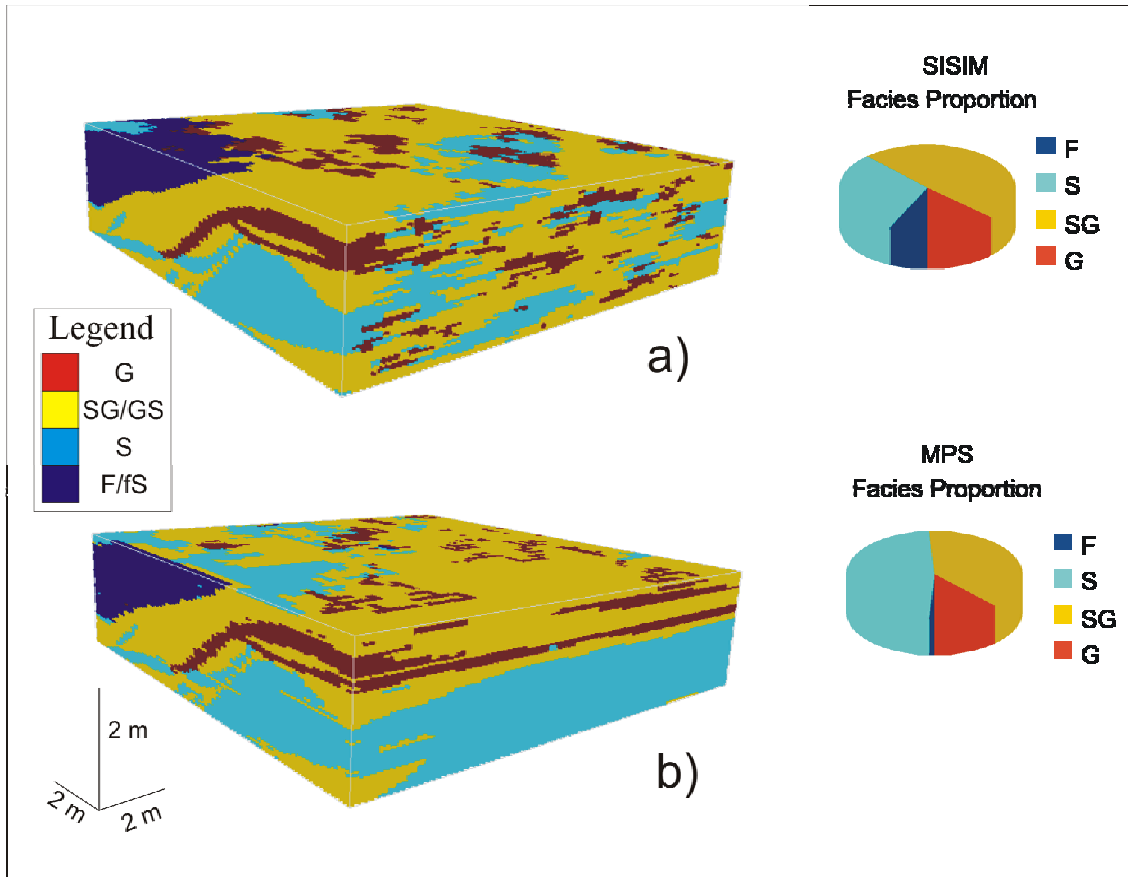


Figure 2: Realisations of the test volume obtained with SISIM (a) and MPS (b). The facies proportions are presented in the pie charts.

3 THE VIRTUAL FLOW AND TRANSPORT EXPERIMENTS AND THE CONNECTIVITY INDICATORS

The equivalent conductivity tensor was estimated for each realization from virtual flow data obtained with a finite differences conservative scheme^{15,5,9,10}.

Virtual transport experiments were conducted with a particle tracking technique, simulating the convective transport of a non reactive (or conservative) solute in a steady flow field¹⁴: no diffusion is considered at fine scale, so that dispersion at the scale of the depositional units (A and B) is the effect of the heterogeneity of the flow field at the hydrofacies scale. Average ground water flow is along the WE direction, perpendicular to the widest conditioning face: Dirichlet boundary conditions are assigned on the borders perpendicular to the average flow direction and are such that a unit average hydraulic gradient occurs, whereas no flow boundary conditions are assigned on the borders parallel to the average flow direction.

The results of the virtual flow and transport experiments were used to assess not only hydrodynamic (equivalent conductivity) or hydrodispersive (apparent or effective dispersion

tensor) parameters, but also to estimate some connectivity indicators.

In fact, among the great number of statistics proposed in the scientific literature to quantify connectivity (a thorough review can be found elsewhere¹⁴), in this work the following flow and transport connectivity indicators¹² are considered: CF_2 is the ratio between the geometric mean of the conductivity and K_{xx} , the equivalent conductivity along the average flow direction; $CT_1 = \bar{t}/t_{5\%}$, where \bar{t} is the average travel time of the contaminant plume and $t_{5\%}$ is the travel time at which the 5% of the solute plume exits from the outflow face of the block.

Moreover, the ensembles of equiprobable realizations are used also to estimate the stochastic properties of the indicators of facies connectivity¹⁴. The total, normal and intrinsic facies connectivity (C^t , C , C^*) provide different information, since the latter is less influenced by the amount of the relative facies. Moreover both omnidirectional and directional indicators can be computed: for this study the directional connectivities are computed along the average flow direction of the virtual transport experiments.

4 RESULTS

The equivalent conductivity tensor showed an anisotropy between the vertical direction and the horizontal plane. The frequency distribution of K_{xx} is represented in figure 3. It is clear a difference between the two methods of geostatistical simulations; in fact the values of K_{xx} for MPS are greater than those for SISIM.

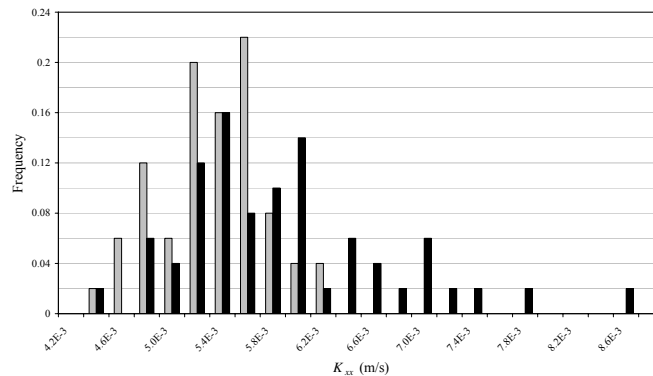


Figure 3: Frequency distribution of K_{xx} for the ensembles of 50 equiprobable simulations obtained with SISIM (gray bars) and MPS (black bars).

The analysis of the total connectivity (figure 4) quantitatively confirms the remark that arises from the visual inspection of the realisations (see the examples shown in figure 2): the dominant facies is SG for SISIM and S for MPS. This difference is apparent also for CT_1 , but not for CF_2 (see figure 5).

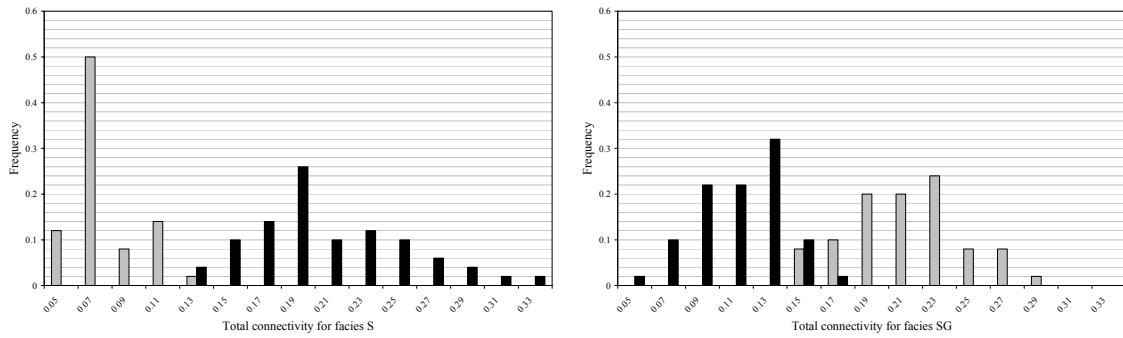


Figure 4: Frequency distribution of the total connectivity of facies S (left) and SG (right) for the ensembles of 50 equiprobable simulations obtained with SISIM (gray bars) and MPS (black bars).

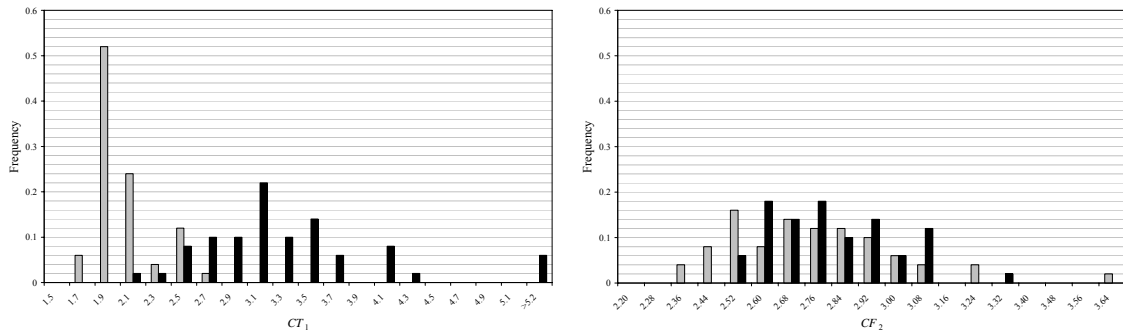


Figure 5: Frequency distribution of CT_1 (left) and CF_2 (right) for the ensembles of 50 equiprobable simulations obtained with SISIM (gray bars) and MPS (black bars).

Other information on the characteristics of the different simulation methods can be obtained from the analysis of the correlation of the flow and transport equivalent parameters (K_{xx}) or connectivity indicators (CT_1 , CF_2) with the indicators of facies connectivity. The standard correlation coefficient, ρ , was used to quantify the link between different quantities: significant values were obtained in few cases. However the following remarks should be stressed.

For SISIM, K_{xx} is weakly correlated with C^t and C mainly for the S facies ($\rho \approx 0.5$) and to a less extent for the SG and G facies ($\rho \approx 0.4$ and 0.25 , respectively). On the other hand, for MPS, K_{xx} is correlated with C^t and C for the G facies ($\rho \approx 0.85$) and weakly correlated with C^t and C for the S and SG facies ($\rho \approx 0.5$ and 0.24 , respectively).

CT_1 is not correlated with the C^t , C and C^* for the SISIM simulations; in fact, the greatest values of ρ are close to 0.2 for the G facies. The correlation of CT_1 with the indicators of connectivity of the G facies for MPS ($\rho \approx 0.3$) is slightly greater than that for SISIM.

CF_2 is weakly correlated with C^t and C for the SG ($\rho \approx 0.4$) and S ($\rho \approx 0.25$) facies for the MPS simulations, whereas it is correlated with C^t and C for the F facies ($\rho \approx 0.6$) for the SISIM simulations.

5 CONCLUSIONS

Some differences between the two sets of geostatistical simulations are clearly shown from the analysis both of the frequency distributions of K_{xx} , C^t , CT_1 and of the correlation coefficients between different quantities. The two kinds of comparisons yield coherent results.

The greater percentage and connectivity of the G facies for MPS than for SISIM, with a predominance of the SG facies for SISIM and of the S facies for MPS (see figure 4), justifies the fact that K_{xx} attains greater values for MPS than for SISIM and also the correlation between K_{xx} and C^t and C . The remark about the different percentage and connectivity of the G facies between the two simulation ensembles justifies also why CT_1 is only weakly correlated with the connectivity indicators of the G facies for MPS simulations. The fact that CF_2 is correlated with the F facies for the SISIM simulations is related to the fact that the geometric mean of K is quite sensitive to the small values.

As a general final remark, no single connectivity indicator revealed itself apt to completely characterize the transport processes in such a kind of alluvial aquifer, but a comprehensive analysis of different connectivity indicators could give useful insights.

The research is now aiming at extending these results through the computation of the equivalent longitudinal dispersion coefficient and the dispersivity.

ACKNOWLEDGEMENTS

Financial support to this work derived from MIUR and Università degli Studi di Milano through the research project of national interest “Integrated geophysical, geological, petrographical and modelling study of alluvial aquifer complexes characteristic of the Po plain subsurface: relationships between scale of hydrostratigraphic reconstruction and flow models” (PRIN 2007: PI M. Giudici). The owner company of “Ca’ de Geri” quarry is warmly acknowledged for kindness and hospitality.

REFERENCES

- [1] D. dell’Arciprete, *Caratterizzazione di un analogo di acquifero fluviale meandriforme*, Università degli Studi di Milano, Degree’s thesis (2005).
- [2] D. dell’Arciprete, *Connectivity, flow and transport models in a point bar-channel aquifer analogue*, Università degli Studi di Milano, PhD thesis (2010).
- [3] D. dell’Arciprete, F. Felletti and R. Bersezio, “Simulation of fine-scale heterogeneity of meandering river aquifer analogues: comparing different approaches”, *Geoenv2008* volume, Springer, in press (2009).
- [4] D. dell’Arciprete, R. Bersezio, F. Felletti, M. Giudici and C. Vassena, “Simulation of heterogeneity in a point-bar/channel aquifer analogue”, *Mem. Descr. Carta Geol. d’It.*, in press (2010).
- [5] R. Bersezio, A. Bini and M. Giudici, “Effects of sedimentary heterogeneity on groundwater flow in a quaternary pro-glacial delta environment: joining facies analysis and numerical modelling”, *Sediment. Geol.*, **129**, 327-344 (1999).
- [6] R. Bersezio, M. Giudici and M. Mele, “Combining sedimentological and geophysical data for high resolution 3-D mapping of fluvial architectural elements in the Quaternary

- Po plain (Italy)”, *Sediment. Geol.*, **202**, 230-247 (2007).
- [7] S. F. Carle, G. E. Fogg, “Transition probability-based indicator geostatistics”, *Math. Geol.*, **28**, 453-477 (1996).
- [8] C. Deutsch and A. Journel, *GSLIB: Geostatistical Software Library*, Oxford University Press (1992).
- [9] F. Felletti, R. Bersezio and M. Giudici, “Geostatistical simulation and numerical upscaling to model groundwater flow in a sandy-gravel, braided river aquifer analogue”, *J. Sediment. Res.*, **76**, 1215-1229 (2006).
- [10] M. Giudici and C. Vassena, “About the symmetry of the upscaled equivalent transmissivity tensor”, *Math. Geol.*, doi:10.1007/s11004-007-9101-0 (2007).
- [11] P. Goovaerts, *Geostatistics for Natural Resources Evaluation*, Oxford University Press (1997).
- [12] C. Knudby and J. Carrera, “On the relationship between indicators of geostatistical, flow and transport connectivity”, *Adv. Water Resour.*, doi:10.1016/j.advwatres.2004.09.001 (2005).
- [13] S. Strebelle, “Conditional simulation of complex geological structures using multiple point statistics”, *Math. Geol.*, **34**, 1-22 (2002).
- [14] C. Vassena, L. Cattaneo and M. Giudici, “Assessment of the role of facies heterogeneity at the fine scale by numerical transport experiments and connectivity indicators”. *Hydrogeol. J.*, doi:10.1007/s10040-009-0523-2 (2009).
- [15] C.D. White and R.N. Horne, “Computing absolute transmissivity in the presence of fine scale heterogeneity”, *Soc. Pet. Eng.*, **16011**, 209–221 (1987).